materials

Article

Effect of Stitching, Stitch Density, Stacking Sequences on Low-velocity Edge Impact and Compression after Edge Impact (CAEI) Behavior of Stitched CFRP Laminates

Jiamei Lai [1], Ze Peng [1], Zhichao Huang [2,*], Meiyan Li [1], Mingzhi Mo [1] and Bangxiong Liu [1]

[1] Polymer Processing Research Laboratory, School of Advanced Manufacturing, Nanchang University, Nanchang 330031, China; laijm@163.com(J.L.); pz18271660785@163.com(Z.P.); 18870056931@163.com(M.L.); arctan60@126.com(M.M.); liubangxiong0798@126.com(B.L.)
[2] Key Laboratory of Conveyance and Equipment, Ministry of Education, East China Jiaotong University, Nanchang 330013, China; hzcosu@163.com(Z.H.)
* Correspondence: hzcosu@163.com

Abstract: Low-velocity edge impact and compression after edge impact (CAEI) behavior of stitched carbon fiber reinforced plastic (CFRP) laminates was experimentally investigated in the paper. Five groups, including three stacking sequences (P_1,P_2,P_3) and two stitch density(stitch space × stitch pitch is 10 mm×10 mm and 15 mm×15 mm) of stitched/unstitched CFRP laminates were prepared by the VARTM technique and subjected to low-velocity edge impact and compression after edge impact experiments. The damage of CFRP laminates was detected by optical observation and Micro-CT. The effects of stitching, stitch density, stacking sequences and impact energy on properties of edge impact and CAEI were discussed. The results show that the damage of edge impact of stitched laminates is smaller than that of an unstitched laminates. The main failure mode of CAEI of the unstitched laminates is delamination and that of the stitched laminates is global buckling. The addition of stitches can effectively improve the edge impact resistance and damage tolerance of CFRP laminates. Compared with the unstitched laminates with the same stacking sequence, the peak impact force of the laminates with stitch density 15 mm×15 mm increases by 5.61%-12.43%, and the increase of residual compression strength is up to 5-20.9%. The peak impact force of the laminates with stitch density 10mm×10 mm increases by 8.1%-31.4%, and the increase of residual compression strength is up to 24.2-27%. Compared with the other two stacking sequences (P_1 and P_2), the stacking sequence P_3 has the excellent resistance of edge impact and CAEI properties.

Keywords: stitched CFRP laminates; edge-impact; compression after edge impact(CAEI); Micro-CT

Citation: To be added by editorial staff during production.

Received: date
Accepted: date
Published: date

1. Introduction

Carbon fiber reinforced plastics(CFRP) have been widely used in various aerospace structures because of its excellent properties such as lightweight and high-strength[1-2]. However, it is subjected vulnerably to the impact of foreign objects, such as accidental tools dropping in the process of aircraft operation or maintenance or small stones splashed on the platform during takeoff. The impacts, which come from different angles with different energies, may cause serious damage to the composite aircraft structure and result in a significant reduction in its residual strength [3-5], thus leading to a great threat to the flight safety of the aircraft. Therefore, it is urgent to improve CFRP impact resistance and damage tolerance by exploring the damage and impact properties of CFRP under different impact conditions, and the results can provide reference for the design of aircraft structures.

The stitching is a process that effectively improves the impact resistance of CFRP by adding reinforced fiber sutures along the thickness direction of the laminate, which can improve the interlaminar properties. It is simple and low cost process, which is widely concerned by the composite industry and has good application prospects[6-8]. However, the performance enhancement is only achieved for the vertical impact on the center of composite panels.

By now, the research on impact damage characteristics of composite by domestic and foreign scholars were mostly focused on the vertical impact on the center of the composites panels[9-16]. However, research on the edge impact properties of composite laminates was rare until 2008, when Malhotra[17] proposed the idea that composites near special locations such as the edges of aircraft wings, inspection ports, or the edges of other holes in the aircraft are highly susceptible to edge impact from foreign objects, that scholars gradually began to investigate the edge impact and compression after edge impact performance of composites. According to previous studies, composite laminates may face more severe failure when subjected to edge impact than vertical impact[3,18-28], so it becomes critical to understand the damage mechanism of edge impact and try to improve the edge impact properties of laminates.

Based on the previous research work, the stitching process was introduced to experimental study the edge impact and compression after edge impact of stitched / unstitched composite laminates. The effects of stitching, stitch density, stacking sequence and impact energy were discussed in order to explore the effects of stitching on the edge impact and CAEI properties of CFRP laminates.

2. Experiment

2.1 Material Preparation

The CFRP laminate specimens were prepared in three steps. Firstly, a modified locking stitching method (shown in Figure 1) was used to make the preform of stitched CFRP laminate according to three selected stacking sequences P_1 $[-45/0/90/45/90]_{2s}$, P_2 $[45/90/0/-45/0]_{2s}$ and P_3 $[45/0/90/0/-45]_{2s}$. The material used was CF12-300 carbon fiber fabric and Kevlar 29 stitches with two stitch density 15 mm×15 mm and 10 mm×10 mm (it meant stitch space × stitch pitch is 15 mm×15 mm and 10 mm×10 mm), and the diameter of needle was 2 mm. Secondly, the stitched/unstitched CFRP laminates were prepared by the vacuum assisted resin transfer molding (VARTM) process. The matrix material was R688 epoxy resin and the curing agent was amine H3268, the mixing mass ratio of resin to curing agent was 5:1 and the curing time was 1-2 days. The final thickness of the laminates was about 6 mm. Finally, the laminates were cut into standard impact specimens with a length of 150 mm and a width of 100 mm by the CNC water-jet cutter. A total of five groups of different types of specimens were prepared for this experiment, as shown in Table 1.

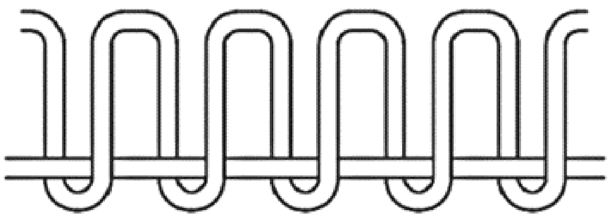

Figure 1. Modified locking stitch method.

Table 1. Types of specimens

Specimen Group	Craft	Stitching Density/(mm)	Stacking Sequence Symbol	Stacking Sequence	Number of Layers	Impact Energy(J)
A	Unstitched	/	P_1	$[-45/0/90/45/90]_{2s}$	20	
B	Stitched	10 ×10	P_1	$[-45/0/90/45/90]_{2s}$	20	
C	Stitched	15 ×15	P_1	$[-45/0/90/45/90]_{2s}$	20	0(no impact)、5、10、15
D	Stitched	15 ×15	P_2	$[45/90/0/-45/0]_{2s}$	20	
E	Stitched	15 ×15	P_3	$[45/0/90/0/-45]_{2s}$	20	

2.2 Edge Impact Tests

In the study, the edge impact test was performed on a drop-weight impact tester CEAST 9340 with reference to ASTM D7136[29], a standard for testing the damage resistance of composite laminates, as shown in Figure 2(a). An edge impact fixture that can be used for edge impact experiments on composite laminates was designed by modifying the existing impact fixture in the laboratory, as shown in Figure 2(b). The edge impact fixture was designed to adapt to the sample size so that the impact point was exactly centered on the long side of the laminates. In order to avoid the difficulty of impact positioning, a wedge impactor was chosen for this experiment. Because it had a certain length, it could be in full contact with the side edge of the laminates in the thickness direction. The total mass of the impactor was 5.5 kg. The drop height of the impactor was automatically adjusted according to the set energy. Impact energy 5 J, 10 J and 15 J were used to conduct edge impact experiments on stitched and unstitched CFRP laminates, and the impact experiments were repeated at least three times for each energy level in this study. The impact response curves were recorded by a data acquisition system DAS 64 K-SC connected to a PC.

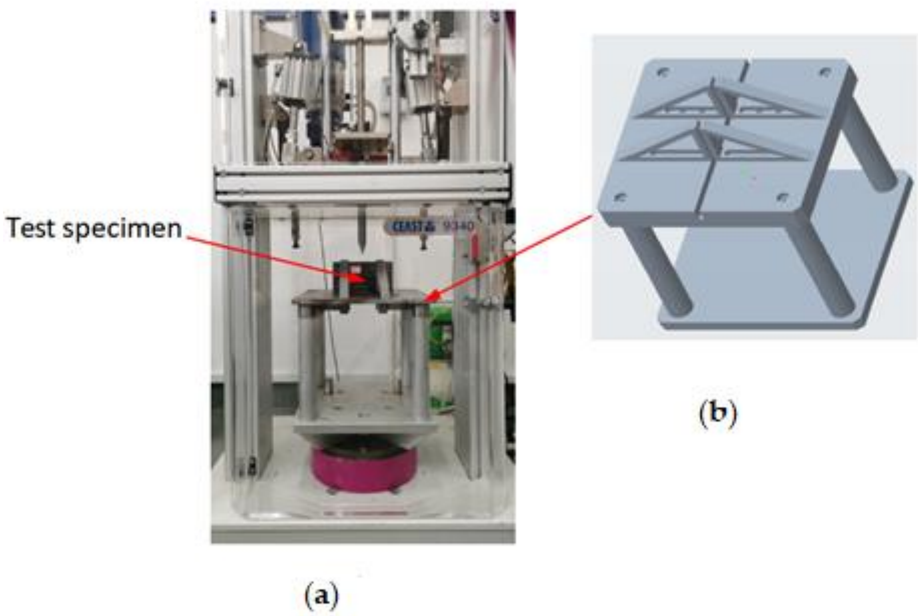

Figure 2. Edge impact test device. (**a**) Drop-weight impact machine; (**b**) Edge impact fixture.

2.3 Compression after Edge Impact Test

The compression after edge impact test was carried out on the ETM105D universal testing machine according to ASTM D7137[30]. To prevent the damage of the specimens caused by edge impact from damaging during the compression clamping process, four 5 mm thick aluminum pads were placed between the laminate and the compression fixture, as shown in Figure 3, and the compression loading speed was 1.25 mm/min.

Figure 3. Compression after edge impact test device.

3. Results Analysis of Impact Response

3.1 Effect of Stitching on Edge Impact of CFRP Laminates

Figure 4 shows the edge impact response results of unstitched CFRP laminates group A, stitched CFRP laminates group B(stitch density 10mm×10mm) and stitched CFRP laminates group C(stitch density 15mm×15mm) at impact energy of 5 J, 10 J, and 15 J, respectively. The specimens of group A, B, C have the same stacking sequence P_1 showed in Table. 1. It is showed in Figure 4(a-b) that at the impact energy of 5 J and 10 J, the impact force-time curves of the stitched and unstitched CFRP laminates have the same trend and the impact forces both show a rapid rise to a peak and then fall back to a certain height with the increase of response time, followed by a period of oscillation up and down near this height plateau, and then gradually decrease to zero. However, when the impact energy is up to 15 J, the change trend of the curve of impact force-time of the laminates is no longer the same. The impact force of the stitched and unstitched CFRP laminates at the impact energy of 15 J shows a continuous shaking upward until it rises to the peak force, and then the curves start to decline gradually. Based on the phenomena observed during the impact test, it can be explained that the fiber fracture and matrix cracking in a laminate may occur immediately while the impactor contacts the laminate when the impact energy is up to a certain level, and then a dent is generated at the impact point, in which many matrix fragments are accumulated. When the impactor continues to apply pressure on the laminates, which is similar to the crushing process of the composite matrix fragments[31], resulting in an oscillating rising region as shown in the Figure 4(c). However, the impact energy of 10 J and below may not be enough to cause matrix cracking in the laminates immediately, and the failure such as matrix cracking and fiber breakage may not occur only until the impact energy is transferred to the interior of the laminates.

Figure 4(d-f) are the edge impact force-displacement curves of group A, B, C CFRP laminates at the impact energy of 5J , 10J and 15J. It can be seen that the change trend of impact force-displacement curves of CFRP laminates is the same as that of impact force-time curves of CFRP laminates shown in Figure 4(a-c).

The peak impact force and maximum impact displacement of group A, B, C CFRP laminates at the impact energy of 5J, 10J and 15J are shown in Figure 5.

The peak impact force refers to the maximum force can be borne by the laminates at a certain impact energy, and the maximum impact displacement refers to the maximum deformation can be occurred by the laminates at a certain impact energy. It can also be seen from Figure 5(a) that at the same impact energy, the impact peak force of the stitched laminates is always greater than that of the unstitched laminates. Compared with the unstitched structure in group A, the average impact peak force of the stitched laminates in group C increases by 5.61%, 8.38% and 12.43% at the impact energy is 5 J, 10 J and 15 J respectively, while the average maximum impact displacement decreases by 11.2%, 4.1% and 10.7% at the impact energy 5 J, 10 J and 15 J respectively. And the peak impact average force of the stitched laminate in group B increases by 8.1%, 24.6%, 31.4%, and the maximum impact average displacement decreases by 12.5%, 15.6%, and 21.9% at the impact energy 5 J, 10 J and 15 J respectively. It can be seen that stitching can not only increase the maximum impact force of the laminates, but also significantly reduce the maximum impact displacement of the laminates. This is because the integrity and rigidity of the composite laminates can be improved after the introduction of stitches, thus leading to reduce the deformation of the laminates at the same impact energy.

With the increase of impact energy, the effect of the stitching of the CFRP laminates on the decrease of the maximum impact displacement and the increase of the peak impact force has an obvious increase trend. This shows that the addition of the stitching process is conducive to improving the edge impact performance of CFRP laminates. The stitched laminates can bear more edge impact force than the unstitched laminates at the same impact energy, and the smaller deformation of the stitched laminates lead to smaller damage. After the impact force of the laminates reaches the peak, the force of the stitched laminates drops faster than that of the unstitched laminates, as shown in Figure 4(c). It is more evident when the impact energy is higher than 10J. This is because the introduction of the stitches also causes slight damage of the composite laminates in the stitching process. The stitch resin columns are not only damaged by impact load, and also can also inhibit the expansion of interlaminar delamination during the impact process. The energy absorption and buffering capacity of the stitched laminates are therefore weakened. The higher the impact energy is, the stronger effect of the stitching becomes in the energy ranges above used in the experiment.

Compared the edge impact response results of group B and group C laminates with different stitching density in Figure 4 and Figure 5, it can be found that at the same impact energy, the average peak impact force of group B stitched CFRP laminates is always larger than that of group C stitched CFRP laminates, and the average maximum impact displacement of group B is always smaller than that of group C. It shows that the edge impact resistances of stitch density 10 mm×10 mm stitched CFRP laminates are better than that of stitch density 15 mm×15 mm stitched CFRP laminates. The reason is that the number of internal stitch resin columns in the group C laminates is less than that in the group B laminates, and the increase stiffness of group C laminates is smaller than that of group B laminates. The effect of inhibiting the interlaminar crack propagation of the group C laminates by edge impact is worse than that of group B laminates, resulting in weaker impact resistance of the group C laminates. Therefore, it can be concluded that the denser the stitch density is, the stronger the edge impact resistance of CFRP laminates have. However, this conclusion is only limited to the two stitch density involved in this experimental study. With the continuous increase of the stitch density, whether the edge impact performance of CFRP laminates will continue to increase needs to be further studied by adding more experiments.

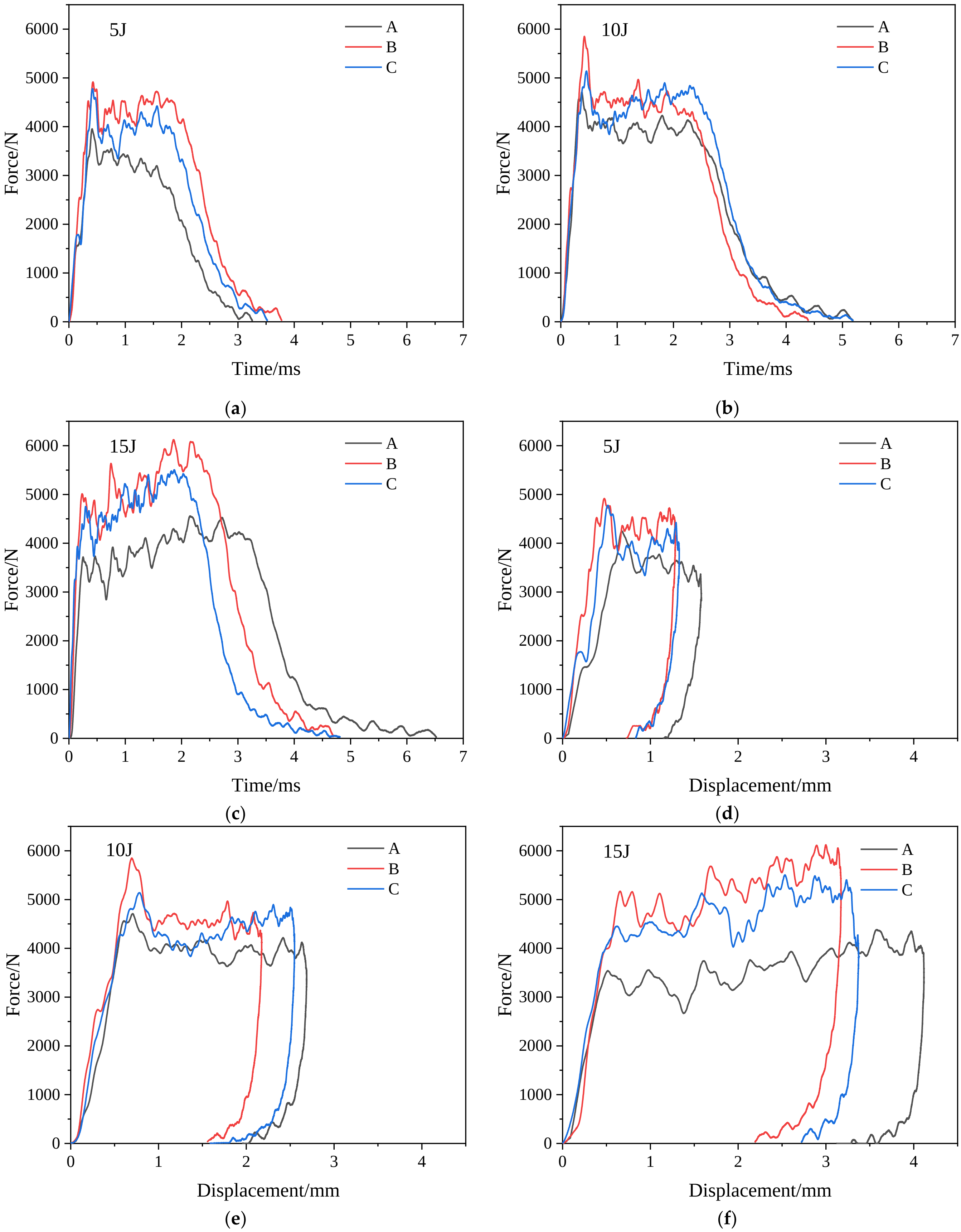

Figure 4. Edge impact response of groups A ,B and C specimens. (**a-c**) Impact force-time curve at impact energy of 5J, 10J, 15J; (**d-f**) Impact force-displacement curve at impact energy of 5J, 10J, 15J.

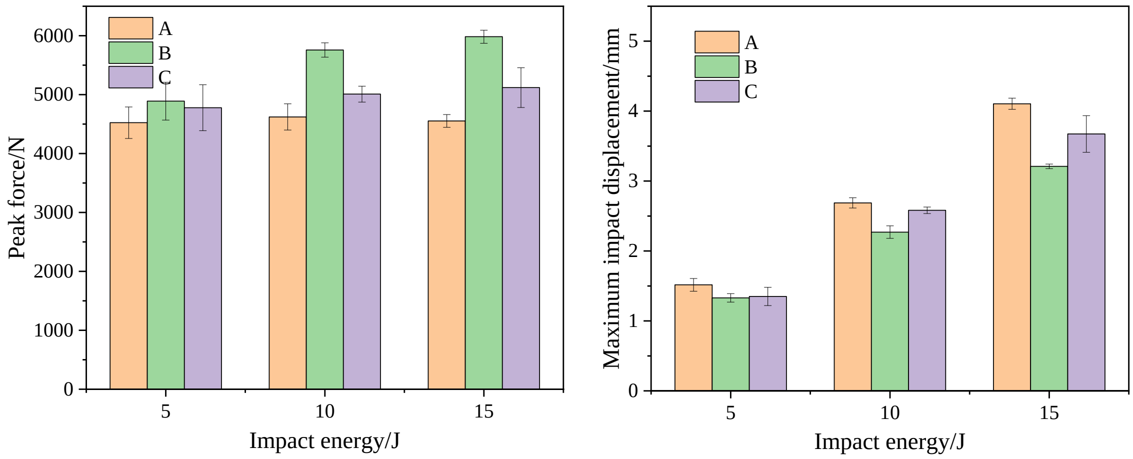

(**a**) (**b**)

Figure 5. Peak impact force and maximum impact displacement of edge impact of specimens groups A ,B and C. (**a**) Peak impact force; (**b**) Maximum impact displacement.

3.2 Effect of Different Stacking Sequences on Edge Impact of CFRP Laminates

Figure 6 shows the edge impact response results of CFRP laminates in groups C, D, and E at the impact energy of 5 J, 10 J and 15J respectively. The corresponding stacking sequences of groups C, D and E are P_1, P_2, and P_3 with the same stitch density 15 mm×15 mm, as shown in Table 1.

Firstly, it can be seen from Figure 6(a-c) that the order of the peak impact forces for the specimens with different stacking sequences at the same impact energy is: $P_3>P_1>P_2$. The group E with the stacking sequence P_3 has biggest the peak impact forces.

During the edge impact process, the impact direction is parallel to the 90° fibers, so the propagation speed of the impact stress along the 90° fiber direction is the fastest. The group C laminates are not only laid with 90° fibers in the middle ply, but also their 90° fibers content is 40%, which is significantly higher than the 90° fiber content of the other two groups of laminates, so the impact stress in group C laminates can be better transferred to the interior of the laminates. As a result, the laminates in group C have more severe damage than those in group E, which causes the lower peak impact force that the group C laminates can bear.

The peak impact force of group D laminates is lower than that of group C laminates probably because their middle plies are laid with 0° fibers, which are perpendicular to the direction of edge impact. When the impactor falls and hits the laminates, the first fracture should occur in the 0° fiber plies. Therefore, during the edge impact experiments, when the middle plies of the Group D laminates with stacking sequence P_2 break, an obvious dent will be occurred immediately below the impact point, followed by rapid propagation of the impact crack, and the laminates will soon be unable to continue to withstand the greater compressive stress of the impactor, and the peak impact force of the group D laminates will be minimal.

Figure 6(d-f) shows the edge impact force-displacement curves obtained from the laminates of groups C, D, and E at the impact energy of 5 J, 10 J and 15J. Table 2 shows the average peak impact force and maximum impact displacement of group C, D and E specimens. Combining the data in Figure 6 and Table 2, it is easy to find that the order of the maximum impact displacement of the laminates of groups C, D, and E is: D > C > E. Group D laminates with stacking sequence P_2 have the worst impact resistance because they suffer the most severe plastic deformation after impact, which their maximum impact displacements are the largest compared to the other two groups of laminates. Group E laminates with stacking sequence P_3 own the best impact resistance and the smallest plastic deformation, the maximum and final displacements after edge impact among the three groups of specimens. This will be illustrated by Figure 7.

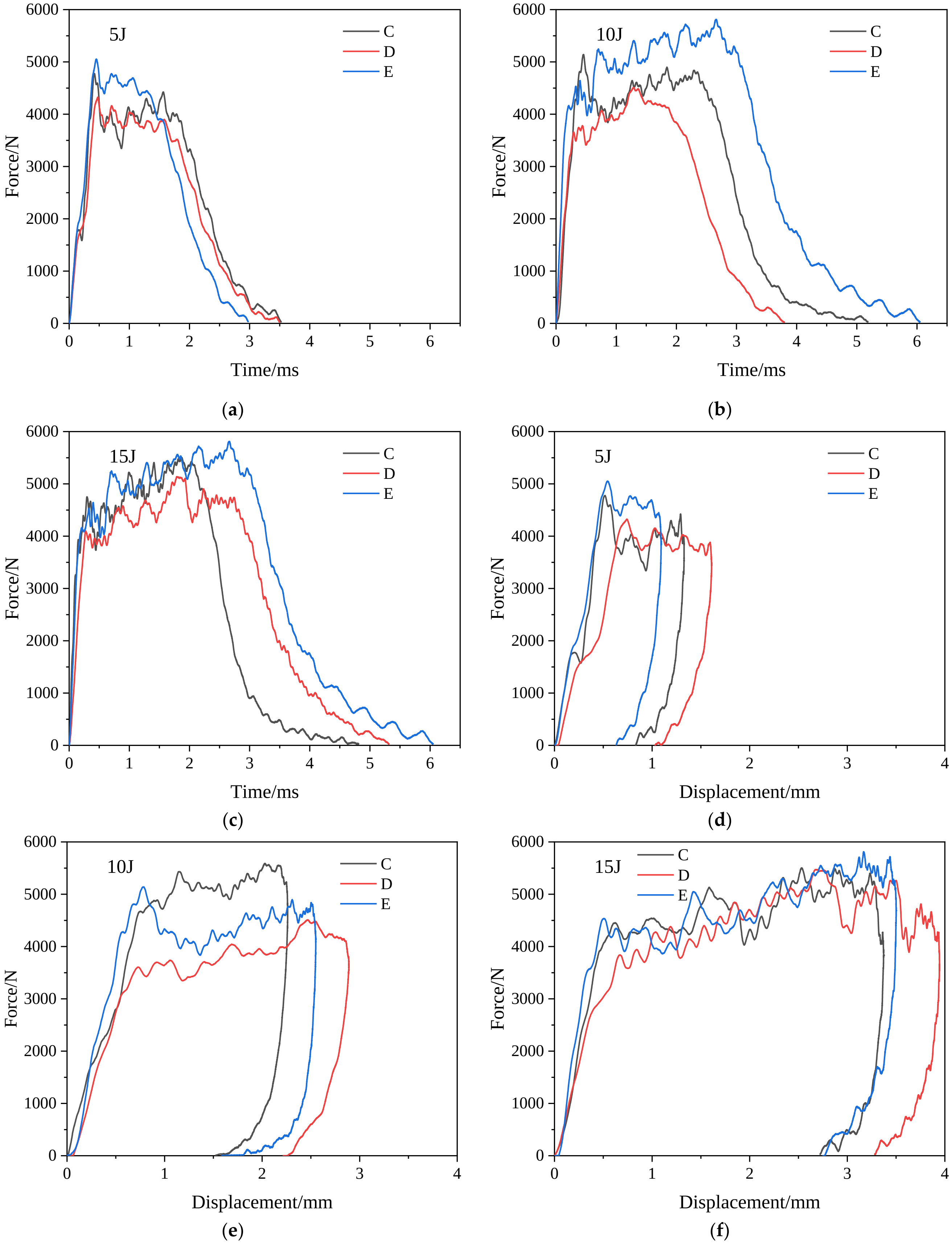

Figure 6. Edge impact response of groups C ,D and E specimens. (**a-c**) Impact force-time curves at under impact energy of 5J, 10J,15J; (**d-f**) Impact force-displacement curves at impact energy of 5J, 10J,15J.

Table 2. Average peak impact force and maximum impact displacement of group C, D and E specimens

Specimen Group	Stacking Sequence Symbol	Impact Energy/(J)	Average Peak Impact Force/(N)	Average Maximum Impact Displacement/(mm)
		5	4777	1.35
C	P_1	10	5009	2.58
		15	5119	3.67
		5	4370	1.36
D	P_2	10	4509	2.62
		15	5329	3.91
		5	5084	1.18
E	P_3	10	5589	2.36
		15	5612	3.61

3.3 Impact Damage Detection

3.3.1 Optical observation

Optical observation is the most common damage detection method of composite aircraft structures after impact, through which the obvious damage such as impact dents, fiber breaks and interlaminar delamination cracks can be found. Visual observation is both convenient and quick. The observed depth of dents on the impact surface of the laminates, the number of fiber breaks and the length of delamination cracks can be as a preliminary judgment basis of the damage degree of structures. In the paper, visual observation was used to examine the damage of the laminates after the edge impact experiments, and to preliminarily compare the damage severity between different specimens.

Figure 7 shows the damage morphology of each group laminates after edge impact at impact energy 5 J, 10 J and 15 J respectively. From the damage shown in Figure 7, with the same stacking sequence laminations (groups A, B and C), compared with stitch density 10 mm × 10 mm (group B), stitch density 15 mm ×15 mm (group C) CFRP laminates, the delamination induced by edge impact in the unstitched CFRP laminates (group A) is the most serious, such as the delamination crack length and crack opening are significantly largest at the same impact energy. This shows that the existence of stitches can improve the rigidity of the composite laminates on the one hand, and inhibit the propagation of delamination cracks on the other. The delamination crack length of group B CFRP laminates is significantly shorter than that of group C laminates at the same impact energy. It can also be found that the dents area of group C CFRP laminates is larger than that of group B laminates, which indicates that the edge impact resistance of group B CFRP laminates with stitch density 10 mm × 10mm is stronger than that of group C CFRP laminate with stitch density 15 mm × 15 mm. This shows that the denser the stitch density is, the greater the effect of inhibiting the propagation of delamination cracks is. In addition, it can also be observed from Figure 7 that the group B CFRP laminate at 10 J energy impact occurs a stitch fracture, because the impact point just falls on the stitch, and the fracture of the stitch indicates that it can help to support the part of the impact energy.

With different stacking sequences (groups C, D and E), the damage of the laminates induced by 5 J energy impact is so little that it is difficult to compare the damage degree by observed dents at the impact point visually. At the impact of 10J energy, there is also no obvious difference in the damage of the CFRP laminates. However, at the impact of 15J energy, the damage of the CFRP laminates with stacking sequence P_3 is significantly smaller than that of the other two stacking sequences of laminates, and the length of the interlaminar delamination crack is significantly shorter than that of the other two groups of laminates. Also the damages of fiber cracks, matrix fracture and the debonding between fiber and resin matrix in group E are less than those in group C and group D, that is, The CFRP laminates with stacking sequence P_3 has the best edge impact resistance performance among the three stacking sequences laminates. These phenomena are consistent with the conclusion drawn from the impact response curves of the laminates shown in Figure 6.

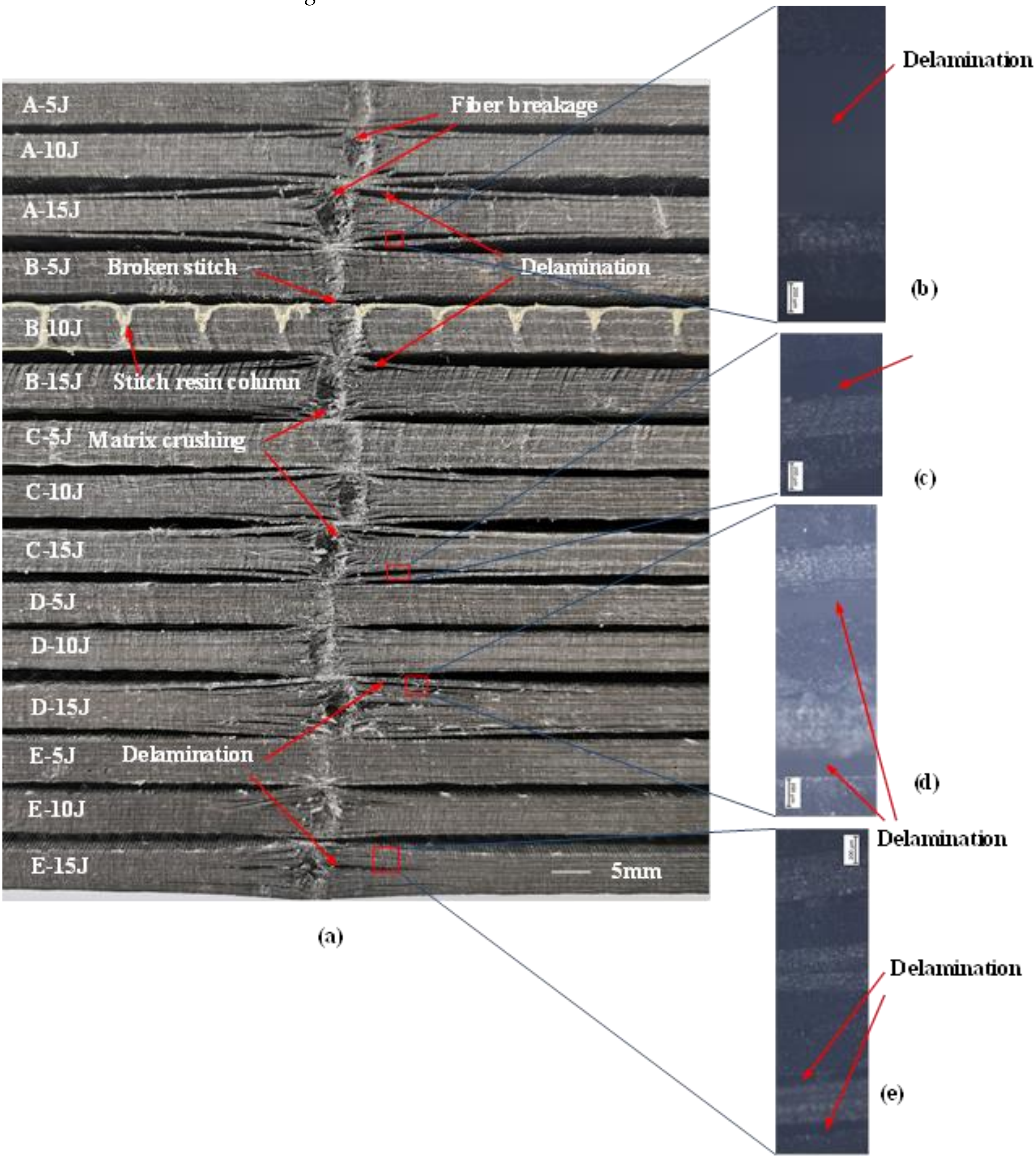

Figure 7. Damage morphology of each group laminates after edge impact at impact energy 5 J, 10 J and 15 J. (**a**) Picture; **(b-e)** Optical microscope picture.

In order to study the delamination details of the laminates, an optical microscope was used to observe the delamination cracks of each laminate, as shown in Figure 7 (b-e). With the same stacking sequence P_1 (groups A, B and C), we found that the main delamination cracks, shown in Figure 7 (a-c), are all located between the 2nd ply and 3rd ply from the surface, that is, the fiber plies are 0^0 / 90^0. The average longest crack length of the impact surface is 66mm in group A, 31mm in group B and 48mm in group C at the impact energy of 15J.

It can be seen from Figure 7 (d) that with the stacking sequence P_2, there are many delamination points. The main cracks are long cracks, which are distributed between the 2nd ply and 3rd ply from the surface, that is, the fiber plies 90°/0°. There are also delamination cracks distributed between the 4th and 5th fiber plies -45°/0° and the 8th and 9th fiber plies 0°/-45°. It can be seen from Figure 7 (e) that with the stacking sequence P_3, the main delamination cracks are distributed between the 7th and 8th fiber plies 0°/90°, and the long cracks are distributed between the 4th and 5th fiber plies 45°/0° from the surface. Therefore, the delamination cracks of the laminates after edge impact mainly propagate along the 0 direction, especially when the fiber plies are 90^0/0^0.

3.3.2 Micro-Computed Tomography

The basic principle of Micro- CT is to perform cross-sectional tomography in the specimen according to the reflection or transmission law after the X-rays are emitted on the specimen surfaces, so as to obtain the two-dimensional cross-sectional image inside the specimen. In this study, the Micro-CT imaging platform was used to perform tomography on the specimens after edge impact. Before CT scanning, a specimen shall be fixed on a transparent PMMA clamp by adhesive tape, and then the clamp and specimen shall be fixed on the test platform in the CT equipment by screws. During CT scanning, the specimen rotates 360° clockwise with the clamp to ensure that all surfaces of the specimen can be scanned. The scanning time of each specimen is about 5 minutes. After the scanning is completed, multiple images of the specimen on three cross-sections of XY, YZ and XZ (the direction of X, Y and Z coordinates is shown in Figure 8) can be obtained respectively.

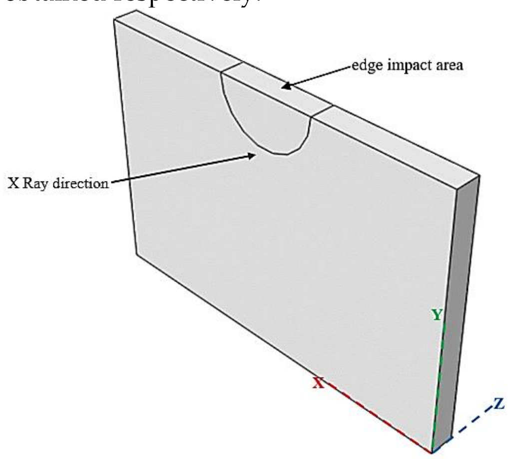

Figure 8. X-ray and specimen coordinate direction.

Because the density at the position of the laminates changes after damage, and the light intensity changes with the different density materials, so the damage of the specimen is characterized by the gray scale of the image in the CT scanning results. Figure 9 shows the damage in XY, YZ and XZ cross-sections of CFRP laminates with unstitched laminates in group A subjected to edge impact of 5J, 15J and stitched laminates in group D subjected to edge impact of 15J.

From the XY cross-sectional view, it can be seen that the specimen has an approximate semi-elliptical damage area below the impact point because the fibers cracks and resin matrix fracture induced by huge compression force from the impactor, while the 0° and ±45° fibers far away from the impact point are subjected to the tensile stress of the laminate itself. From the YZ cross-section of the specimen, it can be seen that there is an approximate "V" shaped damage area in the top of the specimen, and the thickness of the laminates below the impact point has been slightly expanded. From the XZ cross-sectional view of the specimen, it can be found that a lot of interlaminar delamination damage occurs in the laminates, and the delamination cracks extend along the longitudinal direction of the 0° fiber ply from the impact point, especially the delamination damage near the impact surface of the laminates is most serious. That is, the length and width of the delamination cracks are the largest. At the same time, the fibers and resin in the dents are squeezed outward in the thickness direction due to the impact, resulting in an increase in thickness near the impact point.

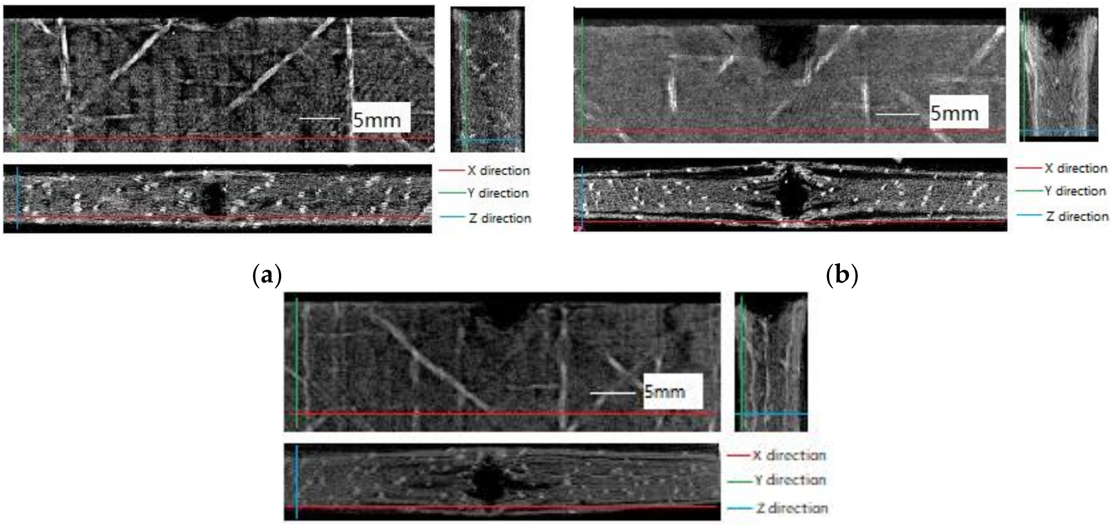

(**a**) (**b**)

(**c**)

Figure 9. Micro- CT scan results of specimens after edge impact. (**a**) A-5J; (**b**) A-15J; (**c**) D-15J.

Compared with Figure 9(a,b), with the increase of impact energy, the area and depth of semi-elliptical dents in the laminates also increase, and the delamination damage is more serious. At the same energy impact, compared with the unstitched laminates shown in Figure 9 (b), the stitched laminates shown in Figure 9 (c) has a significantly less semi-elliptical dents area, depth and the delamination damage, which also shows that stitching can inhibit the propagation of delamination cracks.

The CT technique allows not only to observe the damage of the specimen in each cross-section, but also to specifically observe the damage evolution along a certain coordinate direction. Figure 10 shows the damage evolution images of XZ cross-sections of each group specimens at the impact energy 5J and 15J. In the each graph, because CT scans layer by layer, the first layer is the impact surface, and the corresponding XZ cross-section is taken along the impact direction, that is the negative direction of the Y axis (as shown in Figure 8). The scan spacing is 0.129mm (which is determined by the scanning resolution of the equipment). For example, the nth layer is gone down by (n-1) spacing from the impact surface along the negative direction of the Y axis, which is 0.129 × (n-1) mm. The number of layers of the last image in each group of figures is the deepest layer where the damage reaches, for example, in Figure 10 (f), the deepest damage reaches 0.129× (62-1) = 7.869mm from the impact surface.

It can be found from each group of XZ cross-sections of the laminates that the damage of the specimen gradually decreases from the surface of the laminates to the inside, and extends to a certain depth where no obvious damage can be observed from the CT scan. At the same time, the size of the dents, the length and width of the interlaminar delamination cracks also show gradual decrease from the surface of the laminate to the inside. This is because the gravitational potential energy of the impactor is converted into kinetic energy when it impacts the surface of the laminates. Composite materials absorb the energy brought by impact through deformation, and the energy will decay continuously until it is zero when it is transferred to the depth of materials.

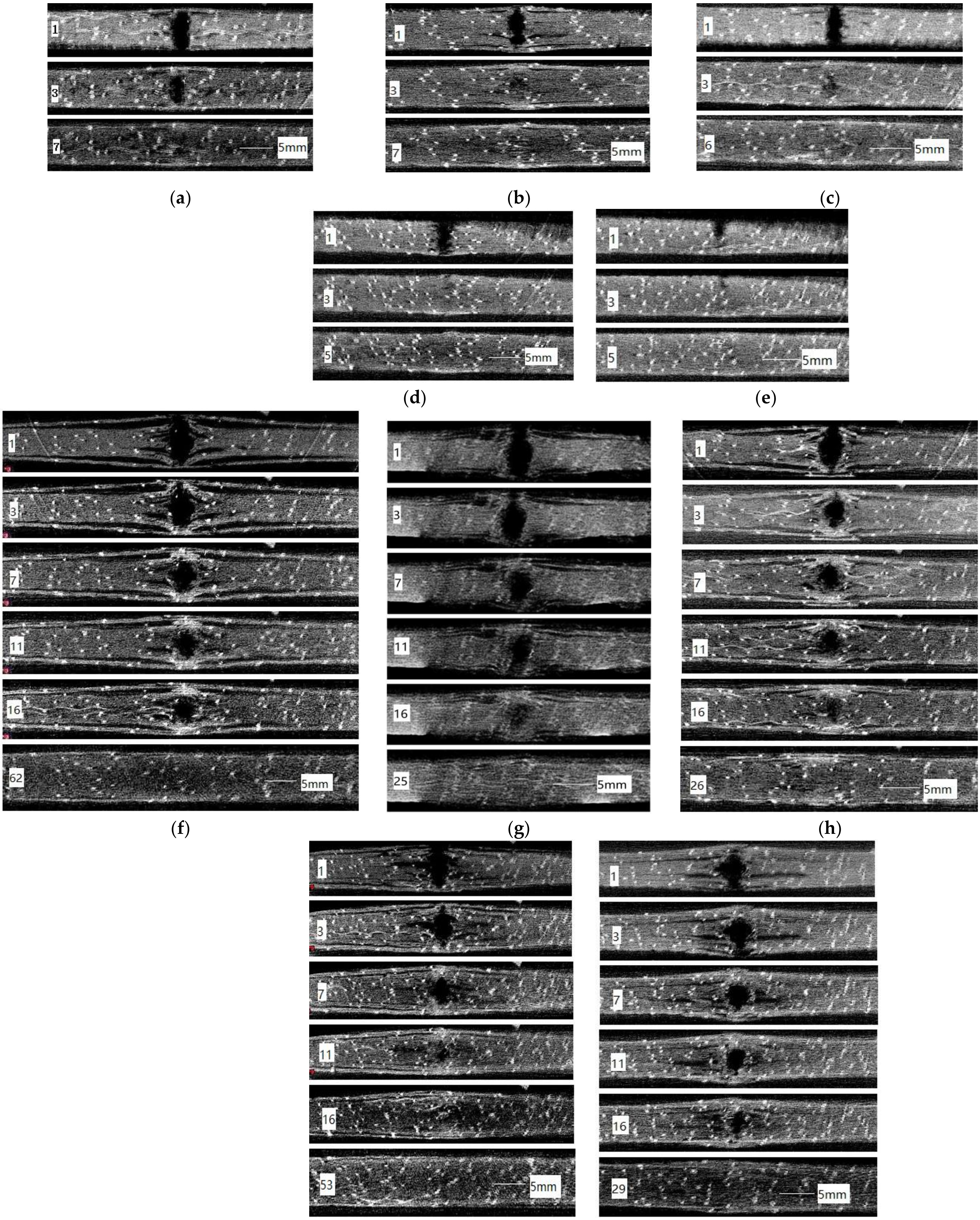

Figure 10. Damage evolution in XZ cross-sections of each group specimens after edge impact at impact energy 5J and 15 J. (**a**) A-5J; (**b**) B-5J; (**c**) C-5J; (**d**) D-5J; (**e**) E-5J; (**f**) A-15J; (**g**) B-15J; (**h**) C-15J; (**i**) D-15J; (**j**) E-15J.

Comparing at the impact energy of 5J shown in Figure 10 (a-e), and at the impact energy of 15J, as shown in Figure 10 (f-j), we can find that the damage of composite laminates in the same group is more serious with the increase of impact energy, and the delamination cracks length, width and crack propagation depth also increase. With the same stacking sequence, at the impact energy of 5J, as shown in Figure 10 (a-c), or at the impact energy of 15J, as shown in Figure 10 (f-h), we can find that the damage of the stitched CFRP laminates (groups B and C) is smaller than that of the unstitched CFRP laminates (group A), and the depth of damage reaches in the laminates is also smaller. It can be seen that the stitch resin columns can also better prevent the damage from propagating to the inside of the laminates.

Moreover, combined with Figure 10 and Figure 7, it can also be found that with the stacking sequences P_1 and P_2, whether the stitched CFRP laminates (group B, C D) or unstitched laminates, the interlaminar delamination between the 2nd ply and 3rd ply near impact surface of the laminates is the most serious, that is, the length and width of the delamination cracks are the largest, while the damage mode of the stacking sequence P_3 (group E) is different from that of the stacking sequences P_1 and P_2.

Combined with Figure 7 (a) and Figure 10 (b-c, g-h), it can be seen that with the same stacking sequence P_1, compared with the group C laminates with stitch density 15 mm ×15 mm, the delamination cracks length of the group B laminates with stitch density 10 mm ×10 mm is much shorter, while the depth of damage is almost the same. It can be showed that the influence of stitch in the X direction is greater than that in the Y direction in the study.

With the same stitch density, whether at impact energy of 5J or 15J, the length and depth of delamination crack of group E laminates with stacking sequence P_3 is smaller than that of group C with stacking sequence P_1 and group D with stacking sequence P_2, while the dents depth of group D is smallest, but the delamination crack reaches a deepest depth, as shown in Figure 10 (c-e) and Figure 10 (h-j).

4. Results Analysis of Compression after Edge Impact

4.1 Compressive Load and Displacement

Figure 11 shows the compressive load-displacement curves of CAEI of the CFRP laminates in groups A ,B ,C after impact of 0J(not-impacted), 5 J, 10 J and 15 J, respectively.

It can be seen that with the increase of compressive displacement, the load changes of the stitched and unstitched laminates are almost the same, they rise rapidly and almost linearly to the peak compressive load and then drop sharply, and the higher the impact energy is, the smaller the peak compressive load and stiffness of the laminates are.

The loss of laminates stiffness increases with the increase of impact energy comparing with the stiffness of not-impacted laminates. The loss of laminates stiffness is very small at impact energy 5J, and the loss of laminates stiffness is the largest at impact energy 15J. This is due to the more serious damage inside the laminates at impact energy 15J, which can be seen in Figure 7 and Figure 10.

The difference is that the initial slope of the compressive load-displacement curve of the stitched laminates is significantly lower than that of the unstitched laminates, which may be due to the fact that the addition of the stitch resin columns blocks the transfer of the fiber compressive stress inside the laminate. There are also some cracks in the stitch resin columns during the impact process, which leads to a linear growth trend of the compressive load of the stitched CFRP laminates only after a certain displacement buffer. Compared with stitched laminates, at the impact energy of 5J, 10J and 15J, the compressive load of unstitched laminates decreases significantly compared with compressive load of the corresponding not-impacted laminates. This is because, as shown in Figure 7 and Figure 10, the greatest damage of unstitched laminates (group A) occurs at the same impact energy.

Figure 11 (b, c) shows compressive load-displacement curves of CAEI of CFRP laminates with stitch density 10 mm × 10 mm of group B and stitch density 15 mm ×15 mm of group C at 0J, 5J, 10J and 15J impact energy. It can be seen that the displacement difference between two kinds of stitch density laminates during CAEI is not large, but the maximum compressive load of group B laminates with stitch density 10 mm ×10 mm is obviously higher than that of group C laminates with stitch density 15 mm× 15 mm. This may be due to the fact that the number of stitch resin columns in the laminates increases when the stitch density increases. More stitch resin columns enhance the longitudinal compressive strength of the laminates, which can help the laminates to withstand greater compression load. It also can be seen in Figure 10 that the damage of group B laminates is smaller than that of group C at the same impact energy.

However, the existence of stitch resin columns will also slightly damage the integrity of the laminates, so increasing the stitch density cannot reduce the compressive failure displacement of the laminates. The maximum displacement of CFRP laminates with two stitch density in the study during compression is similar.

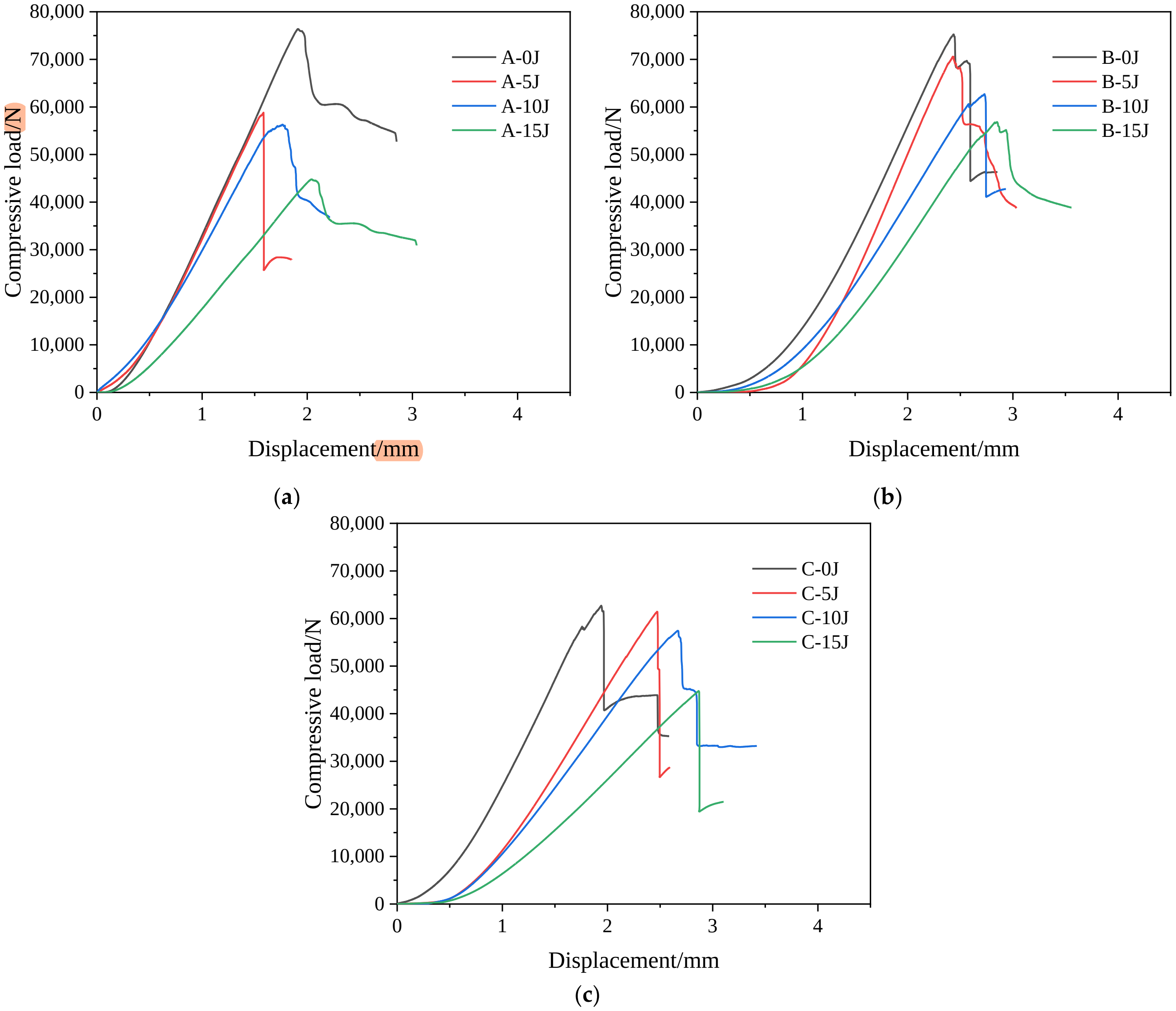

Figure 11. Compressive load-displacement curves of CAEI of groups A ,B ,C laminates. (**a**) Group A; (**b**) Group B; (**c**) Group C.

4.2 The Compression after Edge Impact Failure Mode

It can be found that only the compressive failure modes of stitched and unstitched laminates can be clearly distinguished by observing the CAEI failure modes of CFRP laminates. Figure 12 shows the CAEI failure mode of the unstitched laminates in Group A and stitched laminates in group B.

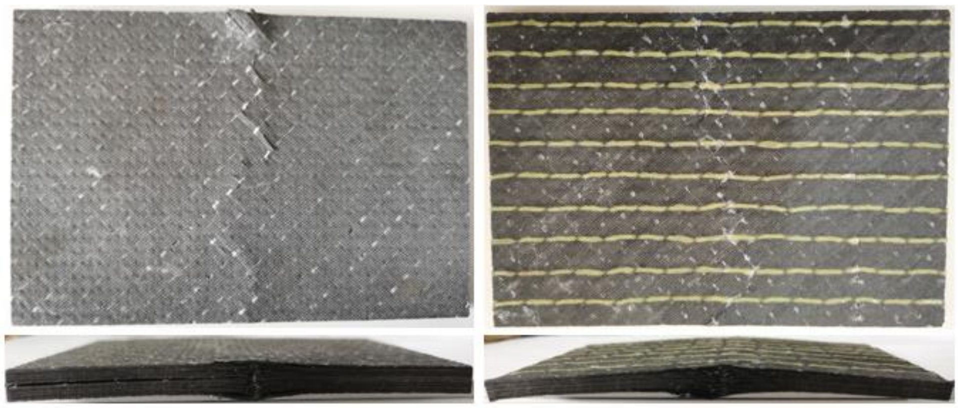

(**a**) (**b**)

Figure 12. Failure mode of CAEI in the laminates. (**a**) Unstitched laminate; (**b**) Stitched laminate.

It can be seen from Figure 12 that after the unstitched specimens are crushed, a long crack perpendicular to the compression loading direction appears in the center of the panel, extending from the impact side to the other side. There is a slight bending of the unstitched laminates. While the stitched laminates show overall buckling, the cracks on the laminate extend along the stitch drop and do not extend to the sides of laminates. Therefore, it is concluded that the main damage mode of compression after edge impact for the unstitched CFRP laminates is delamination and that for the stitched CFRP laminates is overall buckling.

4.3 Analysis of Residual Compressive Strength

The residual compressive strength of each group of stitched and unstitched specimens after edge impact is calculated according to the formula (1) and the curves are drawn as shown in Figure 13.

$$P_{CAEI} = \frac{F_{\max}}{S} \quad (1)$$

In formula (1), P_{CAEI} is the residual compressive strength of the specimen, MPa; $F_{\max}$ is the maximum compressive force of the specimen, N; S is the compressive contact area of the specimen, and $S=b\times h$ (b is the width of the specimen, h is the thickness of the specimen), mm^2.

At the same impact energy, the effect of stitches on residual compressive properties after edge impact can be expressed as [(the average residual strength of stitched laminates − the average residual strength of unstitched laminates)/the average residual strength of unstitched laminates]×100%.

With the same stacking sequence, the residual compressive strength of A, B and C groups of laminates changes with impact energy as shown in Figure 13 (a). Whether stitched or unstitched CFRP laminates, compared with corresponding not-impacted laminates, their residual compressive strength after edge impact will be reduced, but the degree of reduction will be different. At the impact energy of 5 J, 10 J and 15 J, the average residual compressive strength of unstitched CFRP laminates in Group A decreases by 22.9%, 31.5% and 41.3% respectively; The average residual compressive strength of group B CFRP laminates stitch density 10 mm ×10 mm decreases by 16%, 23.7% and 34.8% respectively; The average residual compressive strength of group C CFRP laminates with stitch density 15 mm ×15 mm decreases by 24.1%, 26.1% and 33.5%, respectively. With the increase of impact energy, the average residual compressive strength of each group decreases. This is because the damage caused by edge impact increases with the increase of impact energy, which can be seen in Figure 7, Figure 9 and Figure 10. In addition, at the same impact energy, compared with unstitched laminates, the damage of stitched laminates is smaller, as shown in Figure 9(b, c), and the decrease of the average residual compressive strength is also smaller. Obviously, this is because stitching can inhibit damage propagation when the laminates are subjected to impact.

Compared with unstitched laminates, at 5 J, 10 J, 15 J impact energy, the average residual compressive strength of group C CFRP laminates with stitch density 15 mm ×15 mm increases by 5%, 15% and 20.9% respectively; The average residual compressive strength of group B CFRP laminates with stitch density 10 mm ×10 mm increases by 24.2%, 27% and 26.3% respectively.

This is because the composite laminates have the different damages after edge impact, which are shown in Figure 7, Figure 9 and Figure 10. The damage, especially, the size and depth of dents and delamination damage, of unstitched laminates (group A) is the largest with the same stacking sequence and the same impact energy, which leads to the minimum residual compressive strength. And with the increase of stitch density, the size and depth of dents and delamination damage of group B are smaller than those of group C at the same impact energy, which can be shown in Figure 7 and Figure 10, so the residual compressive strength of group B is higher than that of group C. Therefore, the properties of edge impact and compression after edge impact of stitched laminates are better than those of unstitched laminates. Among the two stitch density involved in this experiment, It can be found that the denser the stitch density is, the stronger properties of the edge impact and compression after edge impact of laminates are.

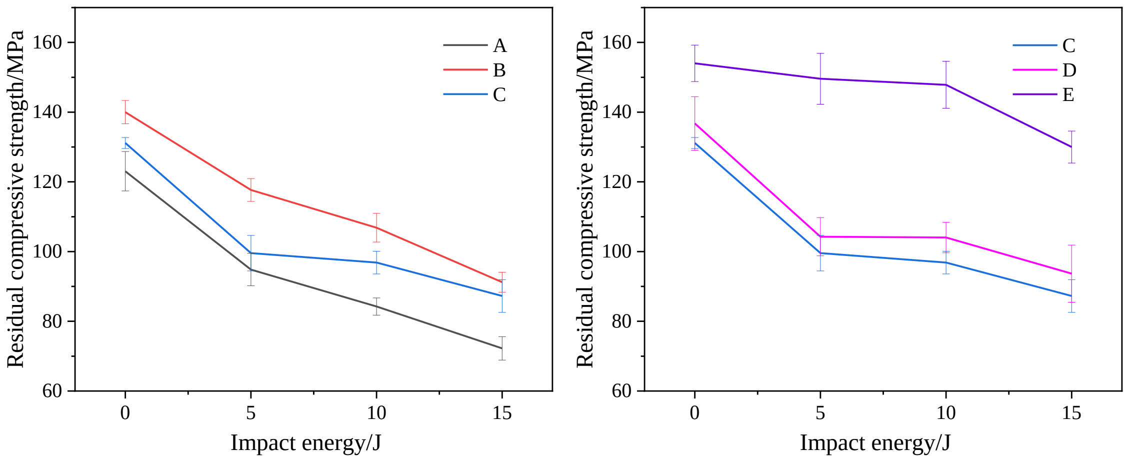

(**a**) (**b**)

Figure 13. Residual compressive strength-impact energy curves of each group laminates. (**a**) Group A, B and C; (**b**) Group C, D and E.

With the same stitch density, the change of residual compressive strength of C, D and E groups of laminates with impact energy is shown in Figure 13 (b). Compared with corresponding not-impacted laminates at the impact energy 5J, 10J and 15J, the average residual compressive strength of group C CFRP laminates with stacking sequence P1 decreases by 24.1%, 26.1% and 33.5% respectively; The average residual compressive strength of group D CFRP laminates with stacking sequence P2 decreases by 23.8%, 23.9% and 31.5% respectively; The average residual compressive strength of group E CFRP laminates with stacking sequence P3 decreases by 2.9%, 4% and 15.6% respectively. Obviously, at the same impact energy, the reduction of the average residual compressive strength of group E CFRP laminates with stacking sequence P3 is the smallest. This is because the damage of group E laminates is the smallest among the three, which can be seen from Figure 7, Figure 9 and Figure 10. Therefore, the decrease of the residual compressive strength of group E is the smallest, and the decrease of the average residual compressive strength of group C and group D is similar, because the damage caused by the edge impact at the same energy is also similar.

4. Conclusions

CFRP laminates will cause damage after being subjected to edge impact, leading to reduce the residual compressive strength of materials. Based on the above research, the following conclusions can be drawn:

(1) Edge impact will cause much irreversible plastic deformation inside the CFRP laminate. The higher the impact energy is, the greater the impact peak force and the maximum impact displacement of the laminates are. The stitching can improve the resistance of edge impact of the CFRP laminates. The improvement effect of the stitching is more significant with the increase of the impact energy which is used in this study. Compared with the unstitched laminates with the same stacking sequence, the peak impact force of the stitched CFRP laminates with stitch density 15 mm×15 mm has an increase of 4.35%-12.43%. The peak impact force of the stitched CFRP laminates with stitch density 10 mm×10 mm has an increase of 8.1%-31.4%.

(2) In this study, the order of the improvement of the edge impact resistance of the stitched CFRP laminates with three stacking sequences is: P_3 $[45/0/90/0/-45]_{2s}$>P_1 $[-45/0/90/45/90]_{2s}$ >P_2 $[45/90/0/-45/0]_{2s}$. Increasing the stitch density can enhance the toughness of the laminates. The CFRP laminates with stitch density 10 mm × 10 mm have stronger edge impact resistance than those with stitch density 15 mm x 15 mm.

(3) The extremely serious fiber fractures, interlaminar delamination, stitch fractures and matrix fragments are visually observed on the surface when CFRP laminates are subjected to the edge impact with energy of 10 J or more. The damage of edge impact of stitched laminates is always smaller than that of an unstitched laminates. The damage area of dents, the number of fiber breakage and the cracks length of interlaminar delamination of the laminates decrease gradually along the impact direction of impactor, but the changes of delamination cracks length from the surface to the interior of the laminate is not as significant as the other two. The cracks length of laminates with stitch density 10 mm × 10 mm is much shorter than that of laminates with stitch density 15 mm × 15 mm and the depth of damage propagation is similar when they have the same stacking sequence P_1; When the laminates have the same stitch density and different stacking sequences P_1, P_2, P_3, the delamination crack damage of group E laminates with stacking sequence P_3 is smaller than that of group C with stacking sequence P_1 and group D with stacking sequence P_2, while the dents depth of group D is smaller, but the delamination crack reaches a deeper depth at the same impact energy.

(4) The main failure mode of compression after edge impact of unstitched CFRP laminates is delamination and that of stitched CFRP laminates is global buckling.

(5) Stitching can inhibit the delamination growth, so it has a significant role in improving the compression performance after edge impact. As the material damage will be caused by edge impact, the residual compressive strength after edge impact of stitched or unstitched CFRP laminates will decrease compared with the compressive strength of corresponding not-impacted laminates, but the degree of reduction will be different. At the impact energy of 5 J, 10 J and 15 J, the average residual compressive strength of unstitched CFRP laminates in group A decreases by 22.9%, 31.5% and 41.3% respectively; The average residual compressive strength of group B CFRP laminates with stitch density 10 mm ×10 mm decreases by 16%, 23.7% and 34.8% respectively; The average residual compressive strength of group C CFRP laminates with stitch density 15 mm ×15 mm decreases by 24.1%, 26.1% and 33.5% respectively.

(6) With the increase of stitch density and impact energy, the influence of stitching on the residual compressive strength after edge impact of composite laminates increases significantly. Compared with unstitched laminates, the average residual compressive strength of group C CFRP laminates with stitch density 15 mm ×15 mm increases by 5%, 15% and 20.9% at 5 J, 10 J, 15 J impact energy respectively; the average residual compressive strength of group B CFRP laminates with stitch density 10 mm ×10 mm increases by 24.2%, 27% and 26.3% at 5 J, 10 J, 15 J impact energy respectively.

(7) With different stacking sequences and the same impact energy, the average residual compressive strength of group E CFRP laminates with stacking sequence P_3 decreases the least. Compared with corresponding not-impacted laminates at the impact energy 5J, 10J and 15J, the average residual compressive strength of group C CFRP laminates with stacking sequence P_1 decreases by 24.1%, 26.1% and 33.5% respectively; The average residual compressive strength of group D CFRP laminates with stacking sequence P_2 decreases by 23.8%, 23.9% and 31.5% respectively; The average residual compressive strength of group E CFRP laminates with stacking sequence P_3 decreases by 2.9%, 4% and 15.6% respectively. The mechanism of excellent impact resistance of stacking sequence P_3 needs to be further studied and revealed.

Author Contributions: (J.L.: Conceptualization, Writing—original draft, Writing—review & editing, Supervision, Project administration; Z.P.: Methodology, Visualization; Z.H.: Funding acquisition, Supervision; M.L.: Resources, Data curation, Investigation; M.M: Investigation; B.L.: Micro-CT experiment, Writing—review & editing. All authors have read and agreed to the published version of the manuscript.

Funding: This research was funded by the National Natural Science Foundation (The contract grant numbers: 51763016) of China.

Institutional Review Board Statement: Exclude this statement.

Informed Consent Statement: Not applicable.

Data Availability Statement: Not applicable.

Acknowledgments: I would like thank the financial support of national Natural Science Foundation of China（Grant number 51763016）. I also acknowledge the experimental support from key laboratory for conveyance and equipment of the ministry of education，East China Jiao Tong University in Nanchang.

Conflicts of Interest: The authors declare no conflict of interest.

References

1. Yang B.; Chen Y.; Lee J.; Fu K.; Li Y. In-plane compression response of woven CFRP composite after low-velocity impact: Modelling and experiment. *Thin-Walled Struct*. **2021**, 158, 107186. https://doi.org/10.1016/j.tws.2020.107186.
2. Duan Y.; Xie X.; Zou T.; Wang T. Mechanical Response of CFRP Laminates Subjected to Low-Velocity Oblique Impact. *Appl. Comp. Mater.***2022**, 29, 1105-1124. https://doi.org/10.1007/s10443-021-10006-z.
3. Ostré B.; Bouvet C.; Lachaud F.; Aboissière J. Edge impact damage scenario on stiffened composite structure. *J. Comp. Mater.* **2015**, 49, 1599-1612. https://doi.org/10.1177/0021998314537325.
4. Tuo H.; Lu Z.; Ma X. Zhang C.; Chen S. An experimental and numerical investigation on low-velocity impact damage and compression-after-impact behavior of composite laminates. Comp. Part B: Eng. **2019**, 167, 329-341. https://doi.org/10.1016/j.compositesb.2018.12.043.
5. Psarras S.; Muñoz R.; Ghajari M.; Robinson P.; Furfari D. Smart Intelligent Aircraft Structures; Springer, Cham 2016; pp. 667-679. https://doi.org/10.1007/978-3-319-22413-8_31.
6. Liu D. Delamination resistance in stitched and unstitched composite plates subjected to impact loading. *J.of Reinf. P. and Comp.* **1990**, 9, 59-69. https://doi.org/10.1177/073168449000900104.
7. Adams D. O.; Stanley L. E. Development and evaluation of stitched sandwich panels, NASA CR-211025 ,Washington, Reports, **2001**, 1- 166
8. Ruan J.; Lai J; Wang S; Huang Z. Compression properties after impact of stitched foam sandwich structure. *Polym. Mater.Sci.Eng.* **2020**, 36, 103-111. https:// doi:10.16865/j.cnki.1000-7555.2020.0172.
9. Staroverov O.; Strungar E.; Wildemann V. Evaluation of the survivability of CFRP honeycomb-cored panels in compression after impact tests. *Frattura ed Integrità Strutturale*. **2021**, 15, 1-15. https://doi.org/10.3221/IGF-ESIS.56.01.

10. Ansari M. M.; Chakrabarti A. Impact behavior of FRP composite plate under low to hyper velocity impact. *Comp. Part B: Eng.* **2016**, 95, 462-474. https://doi.org/10.1016/j.compositesb.2016.04.021.
11. Wang S.; Lai J.; Ruan J.; Hu G.; Huang Z. Low speed impact and compression properties of epoxy based carbon fiber composite modified by different particles. *Mater. Rep.* **2021**, 35, 2178-2184.
12. Singh K. K.; Shinde M. *Impact Behavior of Fibre Reinforced Laminates*. Springer, Singapore, 2022; pp. 265-302. https://doi.org/10.1007/978-981-16-9439-4_9.
13. Seamone A.; Davidson P.; Waas A.M.; Ranatunga V. Low velocity impact and compressive response after impact of thin carbon fiber composite panels. *Intl. J. of Solids and Struct*. **2022**, 111604, (*Article in press*). https://doi.org/10.1016/j.ijsolstr.2022.111604.
14. Falcó O.; Lopes C.S.; Sommer D.E.; Thomson D.; Ávila R. L.; Tijs B.H.A.H. Experimental analysis and simulation of low-velocity impact damage of composite laminates. *Comp. Struct.* **2022**, 287, 115278. https://doi.org/10.1016/j.compstruct.2022.115278.
15. Lin S.; Ranatunga V.; Waas A. M. Experimental study on the panel size effects of the Low-Velocity Impact (LVI) and Compression After Impact (CAI) of laminated composites, Part I: LVI. *Comp. Struct.* **2022**, 296, 115822. https://doi.org/10.1016/j.compstruct.2022.115822.
16. Lin S.; Ranatunga V.; Waas A. M. Experimental study on the panel size effects of the low velocity impact (LVI) and compression after impact (CAI) of laminated composites, part II: CAI. *Comp. Struct.* **2022**, 295, 115824. https://doi.org/10.1016/j.compstruct.2022.115824.
17. Malhotra A.; Guild F. J.; Pavier M. J. Edge impact to composite laminates: experiments and simulations. *J. Mater. Sci.* **2008**, 43, 6661-6667. https://doi.org/10.1007/s10853-008-2863-z.
18. Li N.; Chen P. Failure prediction of T-stiffened composite panels subjected to compression after edge impact. *Comp. Struct.* **2017**, 162, 210-226. https://doi.org/10.1016/j.compstruct.2016.12.004.
19. Malhotra A.; Guild F. J. Impact damage to composite laminates: effect of impact location. *Appl. Comp. Mater.* **2014**, 21, 165-177. https://doi.org/10.1007/s10443-013-9382-z.
20. Thorsson S I; Waas A M; Rassaian M. Numerical investigation of composite laminates subject to low-velocity edge-on impact and compression after impact. *Comp. Struct*. **2018**, 203, 648-658. https://doi.org/10.1016/j.compstruct.2018.06.094.
21. Li N.; Chen P. H. Experimental investigation on edge impact damage and Compression-After-Impact (CAI) behavior of stiffened composite panels. *Comp. Struct*. **2016**, 138, 134-150. https://doi.org/10.1016/j.compstruct.2015.11.060.
22. Thorsson S. I.; Sringeri S. P.; Waas A. M.; Justusson B. P. Experimental investigation of composite laminates subject to low-velocity edge-on impact and compression after impact. *Comp. Struct*. **2018**, 186, 335-346. https://doi.org/10.1016/j.compstruct.2017.11.084.
23. Kashiwagi M.; Miura K.; Sato Y.; Nonaka. Y.; Abe T.; Takagi K. Effects of Edge Impact Damage on Compressive Strength of Carbon-Fiber-Reinforced-Plastic Laminates. *J. of the JPN Soc. for Comp. Mater.* **2018**, 44, 49-53.
24. Ostré B.; Bouvet C.; Minot C.; Aboissière K. Experimental analysis of CFRP laminates subjected to compression after edge impact. *Comp. Struct.* **2016**, 152, 767-778. https://doi.org/10.1016/j.compstruct.2016.05.068.
25. Rhead A. T.; Marchant D.; Butler R. Compressive strength of composite laminates following free edge impact. *Comp.: Part A*, **2010**, 41, 1056-1065. https://doi.org/10.1016/j.compositesa.2009.10.024.
26. Ostré B.; Bouvet C.; Minot C. et al. Finite element analysis of CFRP laminates subjected to compression after edge impact. *Comp. Struct.* **2016**, 153, 478-489. https://doi.org/10.1016/j.compstruct.2016.06.041.
27. Arteiro A.; Gray P. J.; Camanho P. P. Simulation of edge impact and compression after edge impact in CFRP laminates. *Comp. Struct.* 2020, 240, 112018. https://doi.org/10.1016/j.compstruct.2020.112018.
28. Liu J.; Xu Y.; Yi X.; Wei T. Experimental and numerical simulation study on Near-edge/On-edge Low-Velocity impact and residual compressive strength of T300/69 laminates. *Comp. Struct.* **2022**, 280, 114887. https://doi.org/10.1016/j.compstruct.2021.114887.
29. ASTM D7136 Standard test method for measuring the damage resistance of a fiber-reinforced polymer matrix composite to a drop-weight impact event. *Annual book of ASTM standards.***2007**.
30. ASTM D7137 Standard test method for compressive residual strength properties of damaged polymer matrix composite plates. *Annual book of ASTM standards.***2007**.
31. Israr H.; Rivallant S.; Barrau J. J. Experimental investigation on mean crushing stress characterization of carbon–epoxy plies under compressive crushing mode. *Comp. Struct.* **2013**, 96, 357-364. https://doi.org/10.1016/j.compstruct.2012.09.022.